A two meter long straw tube prototype for the FINUDA experiment

L. Benussi, M. Bertani, S. Bianco, F.L. Fabbri, P. Gianotti, M. Giardoni, C. Guaraldo, A. Lanaro, V. Lucherini, A. Mecozzi, L. Passamonti, V. Russo, and S. Sarwar.

Presented by S. Sarwar.

Laboratori Nazionali di Frascati,
Via E. Fermi 40, I-00044 Frascati, Italy.

A prototype using several 10 mm and 20 mm diameter, two meter long aluminized mylar straws has been assembled and tested with a one GeV/c pion beam. While operating with dimethyl ether space resolution, and device systematics have been studied. A simple method for measuring straw eccentricity and correcting for the corresponding systematics has been developed and, once applied, a space resolution better than 40 μm can be reached.

1. Introduction

The FINUDA [1],[2] experiment is planned to have an outer tracking device employing about 2500 straw tubes. The straws have an inner diameter of 15 mm and their length, as determined by the required geometrical acceptance, is greater than 2 m.

In order to investigate the straw tube performance, a prototype array using several two meter long, 10 mm and 20 mm diameter, aluminized mylar straws has been assembled at LNF. The geometrical details of the prototype are shown in fig.1. It employs eight two meter long straws with an inner diameter of 10.00 ± 0.05 mm and four 20.00 ± 0.05 mm diameter straws. The 10 mm straws are arranged in four staggered layers, each containing 2 straws. The layers are staggered by 5.1 mm. The four 20 mm straws are all aligned and placed at ∼ 5 cm from the staggered straws. The used straws [3] have a wall thickness of 0.03 ± 0.01 mm.

Gold plated tungsten wires [4] with a diameter of 0.03 mm have been used as anode. The anode wire is crimped in gold plated copper pins shown in fig.2. The feedthrough as shown in fig.2 consists of an aluminum cylinder which, on the straw side, has an external diameter (tapered by 10 % at the beginning) equal to the straw inner diameter with a tolerance of 0.01 mm. The inner surface of the straw is glued on to feedthrough using a silver–based conductive glue [5]. The endplate side of the feedthrough is externally threaded which when tightened with the corresponding nut permits the feedthrough to move along the axis of the endplate hole while pulling the straw to the required tension. The feedthrough contains an inner delrin body which accommodates the wire pin and provides the gas inlet/outlet for the straws.

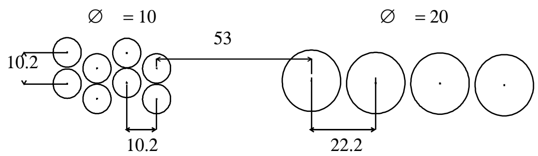

Figure 1. Prototype geometrical details. All dimensions are in millimeters.

During the assembly the wire is initially strung through the straw, feedthroughs, and the pins without any mechanical tension. The inner surface of the straw on the two ends is now glued on to feedthroughs. When the glue is hardened, feedthroughs are inserted in the endplates and the

Figure 3. Circuit diagram of the preamplifier.

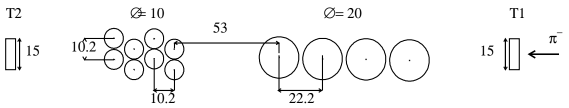

Figure 4. CERN test beam setup. All dimensions are in millimeters.

straw is tensioned to 25 N. After blocking the feedthroughs against the endplates, the wire is crimped inside the pin on one of the straw ends, tensioned to 1 N, and crimped on the opposite end.

The preamplifiers (fig.3) were mounted on printed circuit boards using surface mount devices. The input impedance of the circuit is 300 Ω. Three different preamplifier gain values (1, 2 and 3 V/mA) have been employed on the prototype. The circuit operates with $\pm$ 6 V dissipating 50 mW per channel.

2. Test with pion beam

The prototype was tested with a one GeV/c π^- beam at T10 area of PS (CERN). The test beam setup is shown in fig.4. The 20 mm diameter straws were facing the beam incoming direction followed by 10 mm diameter straws. The straws were operated with pure dimethyl ether (99.8%) at an overpressure of 20 $mbar$. The anode voltage was set to 3200 V for the 10 mm straws and to 3500 V for the 20 mm straws.

A pair of scintillators was used to define a $\sim$ 15×15 mm^2 beam spot. Coincidence of these two gave the start signal to TDCs.

The preamplifiers were mounted immediately after the straw ends. The amplified straw signals were brought to discriminators, operated with a threshold of –30 mV, by 6 m of RG–58 cables. CAEN [6] model N96 discriminators were used for the 10 mm diameter straws whereas CAEN N224 discriminators were employed for the 20 mm straws. The discriminator output was brought to stop input of TDCs by 40 m long RG–58 cables. Drift times were read for both 10 and 20 mm straws using 12 bit TDCs (CAEN C414) operated in common start mode. The TDC full scale was set to 2 μs for 10 mm straws and to 5 μs for the 20 mm straws.

3. Time to space conversion

A typical drift time distribution for 10 mm straws is shown in fig.5. The delay, T_0, due to signal propagation through anode, cables, preamplifier, and discriminator is determined for each channel from the starting edge of the drift time distribution. This value is subsequently subtracted from the read TDC value for all further analysis.

In the ideal case, when the wire and straw centers coincide, the electric field has a cylindrical symmetry and is inversely proportional to the distance from wire. However, due to gravitational and electrostatic forces the wire and straw centers do not coincide. For the prototype straws a maximum eccentricity up to $300 \sim 600$ μm is expected [7].

A simple method can be used to experimentally determine the straw eccentricity. For the test beam data the tracks passing above and below the wire can be separated and the corresponding TDC distributions are shown in fig.6. The straw eccentricity creates an asymmetry in the electric field resulting in zones of low and high field as compared with an ideally concentric straw. The drift velocity is lower than the ideal case for the tracks passing through the low field region (below the wire) and therefore the TDC distribution extends beyond the maximum value for the ideal case. On the other hand, the drift velocity is higher than the ideal case for the tracks passing through the high field region (above the wire) and correspondingly the TDC distribution terminates before the maximum value for the ideal case. The calculated end points of the TDC distribution for the high and low field regions (T^m_{high} and T^m_{low} respectively) as a function of the straw eccentricity are shown in fig.7. In fig.8 the correlation between T^m_{high} and T^m_{low} values for different values of straw eccentricity are shown together with experimental data for different straws and for different values of the beam distance from the straw center. By observing the T^m_{high} and T^m_{low} values, the eccentricity for each straw can therefore be determined (fig.9).

Once the eccentricity is known, the electric field can be computed using the method of images [8]. The field dependence of drift velocity in dimethyl ether as parametrized by [9] is used to compute the time–to–space relationship. The T_0–subtracted TDC values are accordingly transformed into drift distances for the hit straws.

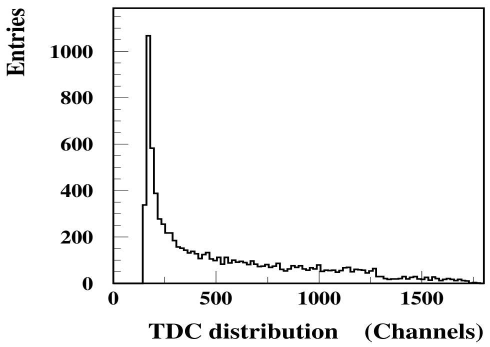

Figure 5. Typical drift time distribution for a 10 mm straw. The starting edge of the TDC distribution determines T_0.

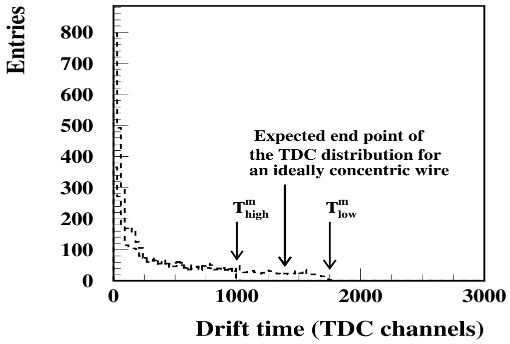

Figure 6. The TDC distributions for tracks passing above (solid histogram) and below the wire (dashed histogram).

4. Space resolution

In order to determine the space resolution for the 20 mm aligned straws one can define a function R_a as:

$$R_a = (r_1 + r_2)/2 - r \quad (1)$$

where r is the drift radius measured by the central straw and r_1,r_2 are the drift radii measured by the two external straws. The rms of the function R_a, denoted by σ_a, is given by:

$$\sigma_a = \sqrt{3/2}\ \sigma(r) \quad (2)$$

where the function $\sigma(r)$ represents the straw *local space resolution* at drift distance r. The depen-

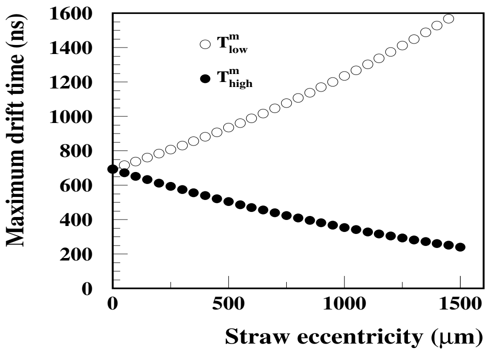

Figure 7. The calculated end point of the TDC distributions for the high and low field zones as a function of straw eccentricity.

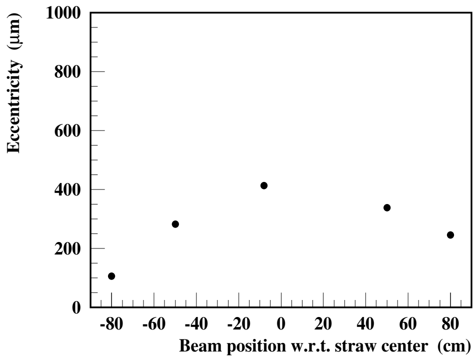

Figure 9. Typical straw eccentricity as a function of distance from the straw center. The eccentricity is determined from the end points of the TDC distributions.

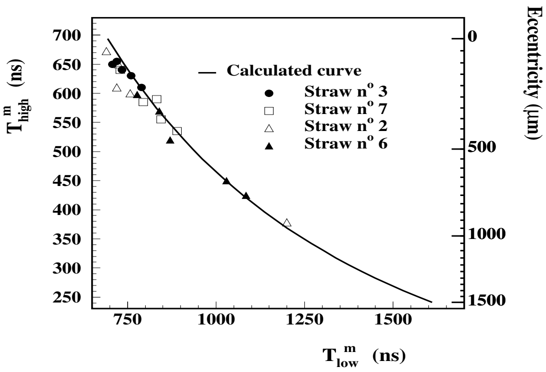

Figure 8. Determination of straw eccentricity from the end points of TDC distributions for the high and low field zones.

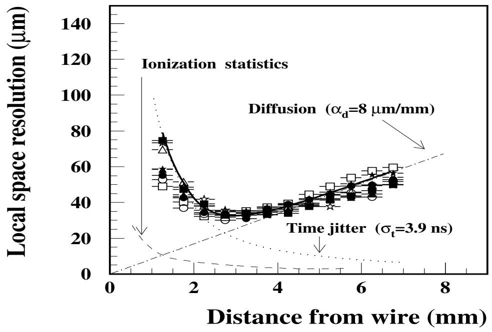

Figure 10. The dependence of local space resolution on drift distance for the 20 mm straws.

dence of the local space resolution on drift distance for the 20 mm straws, as obtained from σ_a values by inverting eq.2, is shown in fig.10. For the major part of the straw radius the local space resolution is smaller than 50 μm, and there is a sharp deterioration in local space resolution as one approaches the wire (smaller drift distances). For drift distance greater than $\sim$3 mm, the local space resolution degrades almost linearly with increasing drift radius. The dependence of local space resolution on drift distance is largely determined by three factors: diffusion of electrons, the variation in the distance between adjacent clusters given by ionization statistics, and jitter in time measurements introduced by used electronics. The detailed considerations of the three contributions are given elsewhere [10] and the solid curve of fig.10 is obtained by fitting the data with a quadratic sum of these three. The individual contributions are also shown in the same figure.

Proceeding in a similar way, a function R_s can be defined for the 10 mm staggered straws:

$$R_s = (r_1 + r_2)/2 + r \qquad (3)$$

The rms of the function R_s, denoted by σ_s, is related to local space resolution $\sigma(r)$ by:

$$\sigma_s = \sqrt{\frac{\sigma^2(\Delta - r)}{2} + \sigma^2(r)} \qquad (4)$$

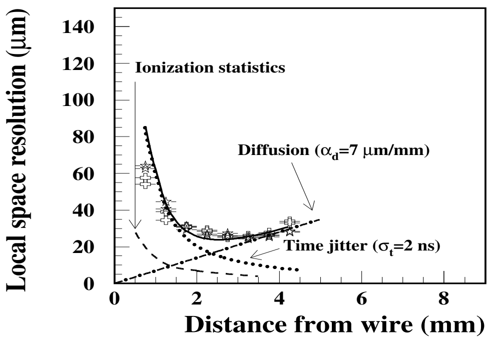

Figure 11. The dependence of local space resolution on drift distance for the 10 mm straws.

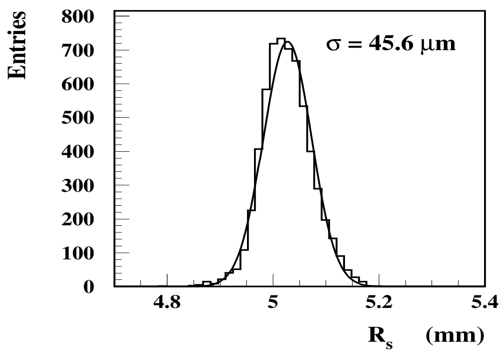

Figure 12. The distribution of the function R_s over the entire straw radius and over different beam positions along the straw axis, for the 10 mm straws.

where Δ (nominally 5.1 mm for the prototype) is the stagger distance between the straws. The local space resolution $\sigma(r)$ for the 10 mm straws is obtained from the σ_s values by inverting eq.4 and is shown in fig.11 along with the contributions due to diffusion, ionization statistics, and time jitter.

A global measure of the straw performance is obtained by considering the the distribution of the function R_s over the entire straw radius and over different beam positions along the straw axis as shown in fig.12. Straw space resolution, defined as $\sqrt{2/3}$ times the rms of the distribution of fig.12, is found to have a value of 37 μm.

5. Conclusions

The first FINUDA straw tube prototype has been constructed and successfully tested for its performance evaluation while operating with pure dimethyl ether.

The dependence of local space resolution on drift distance is found to be in agreement with a simple model considering contributions due to electron diffusion, ionization statistics and jitter in time measurements. The contribution due to electron diffusion is about 7 μm for each mm of drift distance. At drift distances smaller than 2~3 mm, the contribution due to jitter in time measurements dominates the space resolution.

The straw eccentricity is measured from the drift time distributions and the corresponding systematics is corrected. With such a correction procedure, for the first time with 2 m long straws, a space resolution better than 40 μm has been obtained.

REFERENCES

1. M. Agnello et al., LNF report LNF-93/021 (IR). 1993
2. M. Agnello et al., FINUDA Technical Report, (1994 unpublished)
3. Straws were produced by Lamina Dielectrics Ltd. Myrtle Lane, Billingshurst West Sussex England.
4. Wire produced by Luma Metall AB. Box 701. S–391 27 Kalmar Sweden.
5. The conductive glue (type 3M–106) used for the prototype is produced by 3M Italia S.p.A. 20090 Segrate San Felice (MI) Italy.
6. Costruzioni Apparecchiature Elettroniche Nucleari S.p.A. Via Vetraia, 11–55049 Viareggio Italy.
7. L. Benussi et al., FINUDA note ST–04–94 (1994 unpublished).
8. For instance see W. R. Smythe, Static and dynamic electricity (McGraw–Hill, New York, 1950).
9. G. Bari et al., Nucl. Instr. and Meth. A251, (1986) 292
10. L. Benussi et al., FINUDA note ST–02–94 (1994 unpublished).